

1 **Title: Syncytiotrophoblast extracellular vesicles contain functional kynurenine**
2 **metabolising enzymes: potential implications for preeclampsia.**

3
4 Prassana Logenthiran^{1,2}, Toluwalase Awoyemi¹, Morganne Wilbourne¹, Zhanru Yu³,
5 Benedikt Kessler³, Carlos Escudero^{1,4}, Wei Zhang¹, Sofia Cerdeira¹, Manu Vatish^{1*}

6
7 ¹ Nuffield Department of Women's & Reproductive Health, University of Oxford, Women's
8 Centre, John Radcliffe Hospital, Oxford OX3 9DU, United Kingdom

9 ² Department of Physiology, Faculty of Medical Sciences, University of Sri Jayewardenepura,
10 Nugegoda, Sri Lanka

11 ³ Target Discovery Institute, Centre for Medicines Discovery, Nuffield Department of
12 Medicine University of Oxford, Oxford OX3 7FZ, UK

13 ⁴ Vascular Physiology Laboratory, Group of Research and Innovation in Vascular Health,
14 Department of Basic Sciences, Universidad del Bío-Bío, Chillán, Chile.

15
16 *Running title:* Kynurenine is metabolized by syncytiotrophoblast extracellular vesicles.

17
18 *Correspondence: Manu Vatish
19 University of Oxford
20 Nuffield Department of Women's & Reproductive Health
21 Level 3, Women's Centre
22 John Radcliffe Hospital
23 Oxford OX3 9DU
24 manu.vatish@wrh.ox.ac.uk
25

26 **Abstract**

27 **Background:** Placentae of women with preeclampsia (PE) exhibit reduced levels of
28 kynurenine (Kyn), a biological compound derived from tryptophan metabolism with
29 antioxidant, vasorelaxant, and hypotensive properties. Little is known regarding functional
30 levels of the Kyn metabolizing enzymes (KYNME) in women with preeclampsia. Since high
31 circulating levels of syncytiotrophoblast extracellular vesicles (STB-EVs) have been
32 associated with preeclampsia onset, we aimed to study whether Kyn reduction in
33 preeclampsia may be attributed to increased degradation by KYNME present in STB-EVs.

34 **Methods:** We conducted a study that included women with normal (n=9) and early-onset
35 preeclamptic (EOPE) pregnancies (n=9). From them, STB-EVs were isolated by dual-lobe
36 placental perfusions from normal (n=3) and EOPE (n=3). KYNME were identified using
37 placental immunohistochemistry and western blot in placental and STB-EV extractions.
38 Serum Kyn levels were measured using gas chromatography mass spectrometry.

39 **Results:** Cargo of STB-EVs consist of functional KYNME, which break down Kyn in a dose
40 and time-dependent manner. No significant differences in the content of Kyn metabolizing
41 enzymes were found in STB-EVs between normal and EOPE pregnancies. However,
42 decreased serum levels of Kyn were found in women with EOPE relative to normal
43 pregnancies.

44 **Conclusion:** STB-EVs carry functional KYNME and may regulate the levels of circulating
45 Kyn during normal pregnancy and preeclampsia. Due to the dose effect of increased STB-
46 EVs in EOPE, the functional KYNME content of said vesicles may contribute to reduced
47 levels of Kyn. This finding opens a new avenue for investigating the potential benefits of
48 KYNME inhibitors in conjunction with kynurenine replacement for managing preeclampsia.

49
50 **Key words:** Extracellular vesicles; preeclampsia; Kynurenine; Tryptophan; Kynurenine
51 metabolising enzymes

52 **Manuscript word count: 5992**

53 **Abstract word count: 250**

54 **Financial disclosure:** The study was funded by internal contingency funds.

55 **Conflict of interest:** none

56 **Number of figures:** 5

57 **Number of references:** 43

58 **Keycode:** Placenta extracellular vesicles; normal pregnancy; preeclampsia.

59 **Abbreviations:** Chlorotrimethylsilane (TMCS). Comprehensive two-dimensional gas
60 chromatography (GCxGC-MS). Early-onset preeclampsia (EOPE). Extracellular vesicles
61 (EVs). Gas Chromatography Mass Spectrometry (GCMS). International Society for the Study
62 of Hypertension in Pregnancy (ISSHP). Kynureninase (Kynu). Kynurenine (Kyn).
63 Kynurenine aminotransferase III (KAT-III). Kynurenine monooxygenase (KMO).
64 Kynurenine metabolizing enzymes (KYNME). Medium/large syncytiotrophoblast
65 extracellular vesicles (m/ISTB-EVs). N-Methyl-N-trimethylsilyltrifluoroacetamide
66 (MSTFA). Nanoparticle tracking analysis (NTA). Normal pregnancy (NP). Placenta alkaline
67 phosphatase (PLAP). Placental indoleamine 2,3-dioxygenase (IDO). Preeclampsia (PE).
68 Small syncytiotrophoblast extracellular vesicles (sSTB-EVs). Syncytiotrophoblast (STB).
69 Syncytiotrophoblast extracellular vesicles (STB-EVs). Tryptophan (Trp)

70

71

72

73 **Introduction**

74 Preeclampsia (PE) is a multisystem disorder unique to human pregnancy affecting 2% - 8%
75 of pregnancies worldwide^{1,2} and a leading cause of maternal morbidity and mortality^{3,4}. The
76 International Society for the Study of Hypertension in Pregnancy (ISSHP) defines
77 preeclampsia as, *de novo* hypertension (systolic blood pressure, SBP>140mmHg and
78 diastolic blood pressure, DBP>90mmHg) with either new-onset proteinuria, or evidence of
79 other maternal end-organ dysfunction (including liver, kidney, neurological); haematological
80 involvement; or uteroplacental dysfunction⁵.

81 Preeclampsia is thought to originate because of poor placentation^{6,7}. In a pathophysiological
82 context, the clinical syndrome is triggered by the release of placental pro-inflammatory, anti-
83 angiogenic, pro-coagulant factors, and syncytiotrophoblast extracellular vesicles (STB-EVs)
84 as a response to syncytiotrophoblast (STB) stress. These biomolecules mediate maternal
85 endothelial dysfunction, deranged angiogenic balance, vasoconstriction and resultant
86 hypertension, and end organ damage^{6,8}.

87 The syncytiotrophoblast (the outer maternal facing membrane of the chorionic villus) is
88 known to release extracellular vesicles (STB-EVs) into the maternal circulation throughout
89 pregnancy⁹. STB-EVs are membrane bound lipid particles that carry extravesicular proteins
90 and intra-vesicular cargo comprising of lipids, nucleic acids, and proteins, which may play an
91 essential role in the physiological changes accompanying pregnancy¹⁰. STB-EVs are
92 classified based on their size; medium/large STB-EVs (m/ISTB-EVs) are 200 nm to 1 μ m,
93 and small STB-EVs (sSTB-EVs) are ~30-200 nm^{11,12}. m/ISTB-EVs are shed directly from the
94 STB layer via budding of the cell membrane in response to cell activation, cell stress or cell
95 death¹³. In contrast, sSTB-EVs are released from intracellular multivesicular bodies of STB

96 by exocytosis, and they may play a key role in intercellular communication¹⁴. Importantly,
97 women with PE and specially those who present with early-onset PE (PE diagnosed before 34
98 weeks of gestation, EOPE) have shown high quantity of circulating STB-EVs compared with
99 normal pregnancy^{15,16}. Increasing evidence reports that STB-EVs may contribute to the
100 pathogenesis of PE by carrying pro and anti-angiogenic factors as cargoes¹⁷⁻¹⁹.

101 Previous reports have suggested the potential beneficial effects of Kynurenine (Kyn), a
102 biologically active metabolite derived from Tryptophan (Trp) metabolism, in ameliorating
103 detrimental consequences of PE²⁰. Kyn is found to be an antioxidant²¹ a vasorelaxant^{22,23}, and
104 a hypotensive agent²². Kyn has previously been reported to be reduced in placental explant
105 culture medium of PE compared to normal pregnancy (NP)²⁴. Recently, it has been shown
106 that replacing Kyn in pregnant mice with PE-like phenotype induced by uni-nephrectomy
107 was sufficient to improve placental blood flow abnormalities and the PE-like phenotype^{25,26}.
108 These findings prompted the hypothesis that Kyn replacement may serve as a therapeutic
109 intervention to treat the clinical syndrome in PE²⁵.

110 Furthermore, Trp is metabolised by 4 different pathways (serotonin pathway, tryptamine
111 pathway, indole pyruvic acid pathway and kynurenine pathway), but the Kyn pathway
112 accounts for ~95% of overall Trp degradation^{27,28}. The reduction in Kyn in PE was initially
113 attributed to reduced expression of indoleamine 2,3-dioxygenase (IDO) by the placenta, an
114 enzyme responsible for breakdown of Trp to Kyn²⁹. However, the role of the Kyn
115 metabolising enzymes (KYNME)—Kynureninase (Kynu), Kynurenine aminotransferase III
116 (KAT-III) and Kynurenine monooxygenase (KMO)—responsible for breakdown Kyn has not
117 been studied in PE³⁰.

118 We aimed to study whether STB-EVs carry functionally active KYNME and if Kyn
119 reduction in PE may be attributed to increased degradation by KYNME on STB-EVs.

120

121 **Methods**

122 **Human Subjects and Samples**

123 The study received ethical approval from the Central Oxfordshire Research Ethics Committee
124 (RFS 07/H0607/74 & 07/H0606/148). Pregnant women who were scheduled to undergo an
125 elective caesarean section at the Women's Centre, John Radcliffe Hospital in Oxford, were
126 recruited for the study. Before the collection of placentae and blood, written informed
127 consent was obtained from all participants. EOPE was described as outlined above, and the
128 diagnosis was aided with an sFLT-1:PIGF ratio > 85 (n=9), while gestationally matched
129 women with normal pregnancies (NP) were selected based on no history of preeclampsia or
130 hypertensive disorders and sFLT-1:PIGF ratio $< 38^{31}$.

131 Placentae were retrieved in the operating theatre and were perfused within 10 minutes (n=3
132 for both NP and EOPE). Blood samples were collected before caesarean section from NP
133 (n=9) and EOPE (n=9) women in plastic serum tubes (BD Vacutainer, UK) from the left
134 antecubital fossa. These blood samples were then centrifuged (Thermo Multifuge X3R) at a
135 rate of 3,000 RPM for 10 minutes at a temperature of 21°C to separate the serum. The serum
136 was then aliquoted and stored at a temperature of -80°C until analysis.

137 Placental biopsies were collected from the maternal facing surface (without the decidual
138 layer) for protein expression analysis. Placental lysates were prepared using RIPA buffer
139 (150 mM NaCl, 50 mM Tris pH 8.0, 0.1% SDS, 1% Triton X100, 0.5% sodium deoxycholate;
140 ThermoFisher Scientific, UK) and a protease inhibitor cocktail (Sigma Aldrich, UK) and
141 were subsequently subjected to a bicinchoninic acid (BCA) protein assay (Sigma Aldrich,
142 UK). The lysates were then stored at -20°C until analysis.

143 **Enrichment and Characterization of Syncytiotrophoblast Extracellular Vesicles (STB-**
144 **EVs)**

145 STB-EVs were obtained from placentae using a modified ex-vivo dual lobe placental
146 perfusion and differential ultracentrifugation method, as previously detailed by our group³²⁻
147 ³⁵. Placentae were subjected to a 3-hour perfusion process, after which the maternal side
148 perfusate was collected and promptly centrifuged twice using a Beckman Coulter Avanti J-
149 20XP centrifuge and a Beckman Coulter JS-5.3 swing-out rotor. The centrifugation was
150 performed at 1,500 ×g for 10 minutes at 4⁰C to remove large cellular debris. The supernatant
151 was then collected and centrifuged again at 10,000 × g for 35 minutes at 4⁰C to pellet
152 m/ISTB-EVs. The m/ISTB-EVs were suspended in sterile PBS, and the remaining
153 supernatant was filtered through a 0.22 μm Stericup filter (Millipore, UK) and then
154 centrifuged at 150,000 ×g for 125 minutes at 4⁰C. This centrifugation was performed to pellet
155 sSTB-EVs. The sSTB-EVs were then re-suspended in sterile phosphate buffered saline
156 (PBS). The pellets containing m/ISTB-EVs and sSTB-EVs (from the 10K and 150K
157 centrifugations) were assessed for protein concentration using BCA protein assay kit (Sigma
158 Aldrich, UK).

159 **Syncytiotrophoblast Extracellular Vesicles (STB-EV) characterization using**
160 **nanoparticle tracking analysis (NTA), transmission electron microscopy (TEM) and**
161 **western blot**

162 The NanoSight NS500 equipped with a sCMOS camera and NTA software 2.3, Build 0033
163 (Malvern Instruments, UK) was employed to evaluate the diameter and concentration of
164 STB-EVs. The instrument was calibrated with silica 100 nm microspheres (Polysciences,
165 UK). Following calibration, the size profile and concentration of STB-EVs were measured
166 using a standard protocol described in earlier studies³².

167 In addition, sSTB-EVs were characterized by traditional immunoblotting using protein
168 markers specific to sSTB-EVs, such as PLAP, a marker of syncytiotrophoblast origin, and
169 well-known markers of exosomes, including Syntenin, Alix, CD63, and CD9, as
170 recommended by the International Society for Extracellular Vesicles (ISEV). The results of
171 this study confirm the origin of STB-EVs and their classification as exosomes (sSTB-EVs)³⁶.

172 **Transmission electron microscopy (TEM)**

173 STB-EV pellets were resuspended in phosphate-buffered saline (PBS) to achieve a final
174 concentration ranging from 0.1 to 0.3 µg/µl. Suspension (10 µl) was applied to freshly glow-
175 discharged carbon Formvar-coated 300 mesh copper grids. The grids were then negatively
176 stained with 2% uranyl acetate for 10 seconds, followed by blotting and air-drying. Imaging
177 was performed using a FEI Tecnai 12 TEM operating at an acceleration voltage of 120 kV.
178 Images were captured with a Gatan OneView CMOS camera.

179 **Western blot**

180 Immunoblotting was carried out under reducing conditions (except for CD63 performed in a
181 non-reducing condition) and denaturing conditions. Placental lysates (30 µg/well) and
182 m/ISTB-EVs or sSTB-EVs (20 µg/well) were separated by electrophoresis on a 4%-12%
183 SDS-PAGE gel (Thermo Fisher, UK). The proteins were then transferred onto a PVDF
184 membrane (Bio-Rad Laboratories, UK) using a Novex Semi-Dry Blotter (Life Technologies,
185 Paisley, UK). The membranes were blocked for 1 hour at room temperature with 5% (w/v)
186 Blotto (Alpha Diagnostic, UK) in TBS-T (Tris-buffered saline solution with 0.1% Tween-
187 20), and then incubated with primary antibodies, including anti-ALIX antibody ([1 mg/ml] at
188 1:1000 dilution, NBP1-49701, Novus Biologicals), anti-CD63 antibody ([200 µg/ml] at
189 1:1000 dilution, Sc-59286, Santa Cruz Biotechnology), anti-CD9 ([100 µg/ml] at 1:1000
190 dilution, Sc-59140, Santa Cruz Biotechnology), anti-cytochrome C ([200 µg/ml] at 1:1000

191 dilution, Sc-13156, Santa Cruz Biotechnology), and anti-PLAP ([1.67 µg/ml], at 1:1000
192 dilution, NDOG-2, in-house antibody), overnight at 4⁰C. The membranes were washed using
193 TBS-T, and then incubated with horseradish peroxidase (HRP)-conjugated secondary
194 antibodies (Life Technologies, UK) in Blotto/0.1% TBS-T for 1 hour at room temperature.
195 Then, the antigen-antibody complexes were visualized by chemiluminescence using an ECL
196 kit (Thermo Scientific, UK).

197 **Capillary Electrophoresis and Jess Simple Western**

198 Diluted pooled STB-EVs (a mixture of m/ISTB-EVs and sSTB-EVs) obtained from NP (n=3)
199 and PE (n=3) placental perfusion, diluted liver cell lysate [Novus Biologicals, UK; (positive
200 control for KYNME)], and diluted placental tissue lysate (positive control for PLAP) were
201 combined with fluorescent master mix and heated at 95⁰C for 5 min. Protein samples,
202 blocking reagent, target primary antibody, secondary HRP (ready-to-use goat detection
203 module [Jess, Protein Simple], ready-to-use rabbit detection module [Jess, Protein Simple],
204 and ready-to-use mouse detection module [Jess, Protein Simple]), total protein detection
205 reagent, chemiluminescent substrate, and wash buffer were dispensed into designated wells in
206 the manufacturer-supplied microplate. Primary antibodies included goat anti-KYNU [R&D,
207 UK] diluted 1:10, rabbit anti-KMO [R&D, UK] diluted 1:10, rabbit anti-KAT-111
208 [MyBioSource, USA] diluted 1:10, and mouse anti-PLAP [NDOG2 in-house antibody]
209 diluted 1:50. The plate was then loaded into the instrument (Jess, Protein Simple) and
210 proteins were drawn into individual capillaries on a 13 / 25 capillary cassette (12-230 kDa).
211 Data were analysed using the proprietary Compass software provided by the manufacturer.

212 **Immunohistochemistry**

213 The placental tissues obtained from the biopsies were fixed in a solution of 4% formaldehyde
214 (v/v), embedded in paraffin blocks, and then sectioned at a thickness of 10 µm. These

215 sections were placed on slides, and the slides were then processed for histological analysis.
216 Deparaffinized and rehydrated slides were subjected to heat treatment in a solution of 10 mM
217 sodium citrate at pH 6.0 for 10 minutes to facilitate antigen retrieval. Following this, the
218 slides were allowed to cool at room temperature. To block endogenous peroxidase activity,
219 the slides were treated with 3% (v/v) H₂O₂ in phosphate buffered saline (PBS). After that,
220 slides were blocked for non-specific antibody binding with 10% fetal calf serum (FCS)
221 (Sigma Aldrich, UK) in 0.01M PBS-T (PBS with Tween-20) (Sigma Aldrich, UK) at room
222 temperature (1 hour). Placental sections were incubated overnight at 4⁰C with 1% FCS and
223 respective target antibody, including either 1 µg/ml anti-Kynu primary antibody (OriGene,
224 USA); or 1 µg/ml anti-KATIII primary antibody (Santa Cruz Biotechnology, USA); or 1
225 µg/ml anti-KMO primary antibody (MyBioSource, USA) or non-immune mouse IgG1
226 (Biolegend, UK) in PBS-T. The sections were then washed and incubated with α anti-mouse
227 IgG secondary antibody conjugated to horseradish peroxidase (HRP) (Life Technologies,
228 UK) in 10% v/v FCS for 1 hour at room temperature. The slides were then rinsed with PBS-T
229 and stained with DAB (Vector Laboratories, USA). Afterward, hematoxylin solution
230 (Thermo Fisher, UK) was used to stain cell's nucleus. The slides were then observed under a
231 Leica DMIRE 2 microscope. Images were captured using Hamamatsu Orca digital camera
232 and HCI software.

233 **Gas Chromatography Mass Spectrometry (GCMS)**

234 **Sample preparation.**

235 Extraction of metabolites was carried out at room temperature if not indicated otherwise. 800
236 µL of extraction solvent isopropanol (IPA) [1 % trifluoroacetic acid (TFA)] and 2.5 µL
237 myristic acid-14,14,14-d₃ in IPA (1 mg/mL) were added into a bead beater tube with 100 µL
238 of sample. The mixtures were subsequently homogenized in a bead beater (Precellys 24,

239 Bertin Technologies) for three cycles (5000 rpm x 20 s) with dry ice bath between the cycles.
240 Then the mixtures were kept at -80°C for 60 min and were centrifuged (20 min at 13,000g at
241 4°C). The supernatant (aqueous) was collected and transferred into the glass vial to dry under
242 vacuum (Speedvac) overnight.

243 **Chemical derivatization**

244 Chemical derivatization was performed as previously described³⁷. In brief, samples were
245 resuspended in a mixture of 50 μL N-Methyl-N-trimethylsilyltrifluoroacetamide (MSTFA)
246 with 1% chlorotrimethylsilane (TMCS) and 50 μL pyridine. The mixture was then incubated
247 for one hour at 60°C at a shaking speed of 1200 rpm. After incubation, the samples were
248 cooled to room temperature and injected directly for gas chromatography-mass spectrometry
249 (GC-MS) analysis.

250 **Comprehensive two-dimensional gas chromatography (GCxGC-MS) analysis**

251 The samples were promptly analyzed using a GCxGC-MS system, which comprised a gas
252 chromatograph coupled to a quadrupole mass spectrometer (Shimadzu GCMS QP2010 Ultra)
253 and a Shimadzu AOC-20i/s auto sampler, as described previously³⁸. The first-dimension
254 separation was performed on a SHM5MS capillary column (30 m \times 0.25 mm i.d. \times 0.25 μm
255 film thickness, Shimadzu, Japan). The second-dimension separation was carried out on a
256 BPX-50 capillary column (5 m \times 0.15 mm i.d. \times 0.15 μm film thickness, SGE, USA). Helium
257 gas was employed as a carrier gas at a constant inlet head pressure of 73 psi. The modulation
258 period was set to 4 seconds. The samples were injected at a temperature of 280°C in different
259 split ratios of 1:1 or 1:10. The oven temperature was programmed to commence at 100°C and
260 hold for 2 minutes, before increasing to 220°C at a rate of 30°C per minute and holding for an
261 additional minute. The temperature was then raised to 280°C at a rate of 5°C per minute, held
262 for 1 minute, and finally increased to 300°C , where it was held for 2 minutes. The interface

263 temperature between the mass spectrometer and the oven was set at 300⁰C, while the ion
264 source was heated to 230⁰C. The mass spectrometer was operated at scan speeds ranging
265 from 5,000 to 20,000 amu, covering a mass range of 45-600 m/z. Electron Ionization spectra
266 were recorded at an energy of 70 eV.

267 **Data processing and analysis**

268 Raw GCxGC MS data were processed using GCMS solution software (version 2.72/4.20,
269 Shimadzu), and Chromsquare software (version 2.1.6, Shimadzu) in combination with GC
270 Image (version 2.3) and the NIST 11/s, OA_TMS, FA_ME, and YUTDI in-house libraries
271 were used for data analysis. The annotation of kynurenine was carried out by comparing them
272 to external standards, which included IM spectra and retention times adjusted to the internal
273 standard myristic acid-14,14,14-d3. The quantitation of kynurenine was measured using the
274 GCMS Solution software (version 4.2) as accumulated single ion monitoring (m/z 307).

275 **Statistics**

276 Graphs were created, and statistical analyses were conducted using GraphPad Prism
277 (GraphPad Software V10.2.2, Boston, MA, USA). Comparison between the two groups was
278 assessed using Student's paired/unpaired t-test, with a confidence interval of 95%. A *p*-value
279 of <0.05 was considered statistically significant.

280 **Results**

281 **Demographics and clinical characteristics**

282 Table 1 illustrates the demographic characteristics of the women who were studied. As
283 anticipated, women who experienced EOPE displayed significantly higher systolic and
284 diastolic blood pressure, but lower gestational age at delivery, associated with lower birth

285 weight than women with NP ($p < 0.0001$ in all cases). Additionally, the sFlt-1:PIGF ratio was
286 higher in EOPE than NP women (599.3 vs 1.0) ($p < 0.05$). However, no significant differences
287 were observed in maternal age, body mass index (BMI), or gestational age at which blood
288 samples were collected.

289 **STB-EVs characterisation by nanoparticle tracking analysis (NTA), transmission** 290 **electron microscopy (TEM) and western blot (WB)**

291 The results of the NTA revealed that the m/ISTB-EVs extracted from NP placentas were
292 characterized by heterogeneity, with a modal size of 250.8 ± 26.1 nm (Figure 1A). In
293 contrast, the sSTB-EVs exhibited less heterogenic size distribution with a modal size of 169.2
294 ± 8.7 nm (Figure 1B).

295 TEM showed the typical cup-shaped morphology of extracellular vesicles. The 10K STB-EV
296 pellet showed a size heterogeneity characteristic of m/ISTB-EVs (200 to 1000nm) while the
297 150K STB-EV pellet showed a homogeneous EV size profile (less than or equal to 200 nm)
298 (Figure 1A, 1B).

299 The western blot analysis confirmed that both types of EVs expressed the classic STB
300 membrane marker, PLAP, and sSTB-EVs were particularly enriched for ALIX, CD9, and
301 CD63. Furthermore, the results indicated that the m/ISTB-EVs and sSTB-EVs correctly
302 lacked the negative EV marker cytochrome C (Figure 1C).

303 **KYNME expression in placental tissues**

304 Western blot analysis of whole placental lysates obtained from NP (n=3) and EOPE (n=3)
305 exhibited the expression of KYNME including kynureninase (KYNU, 54 kDa), kynurenine
306 monooxygenase (KMO, 59 kDa), and kynurenine aminotransferase III (KAT-III, 59 kDa)

307 (Figure 2A). Liver cell lysate served as the positive control for KYNME. The immunoblot
308 was also probed for PLAP (~66 kDa) to confirm the placental origin of the samples (Figure
309 2A). Qualitative estimation of KYNME found no change between NP and EOPE placental
310 extractions.

311 Additionally, immunohistochemistry was used to confirm the expression of KYNME in the
312 placenta, and the stromal-vascular bed (STB layer) exhibited intense KYNME staining in
313 both EOPE and NP placental tissues (Figure 2B). Again, qualitative estimation of KYNME in
314 the placental immunodetection showed no differences between NP and EOPE.

315 **KYNME expression in STB-EVs**

316 We sought to identify KYNME expression in pooled STB-EVs (mixture of m/STB-EVs and
317 sSTB-EVs) obtained from ex-vivo dual lobe placental perfusion of NP (n=3) and EOPE
318 (n=3) using capillary electrophoresis and western blot. Liver cell lysate and placental lysate
319 were used as the positive controls for KYNME and PLAP, respectively. Surprisingly, all
320 samples (NP and EOPE) tested positive for all three KYNME markers (KYNU, KMO, and
321 KAT-III) and co-expressed PLAP (see Figure 3A). Simultaneous total protein analysis was
322 conducted to ensure accurate results, and the Compass software was utilized to analyze the
323 normalized observed band densities. The variations in KYNME expression between NP and
324 EOPE samples were not statistically significant (see Figure 3B).

325 **Functional assessment of KYNME expressed in STB-EVs**

326 We sought to investigate the functional capacity of the KYNME expressed in STB-EVs (Fig
327 4) by measuring levels of kynurenine using GCxGC-MS. Kynurenine solution was treated
328 with varying amounts of STB-EVs (1 μ g and 5 μ g of total protein) and two different

329 incubation periods (5 min and 60 min). As a control, the kynurenine solution was incubated
330 with STB-EVs treated with 100% trifluoroacetic acid to denature the protein cargo.

331 The results showed that both 1 µg and 5 µg of STB-EVs reduced the kynurenine levels by
332 ~80% and ~90% respectively, compared to the control condition, ($p < 0.05$ for both 1 µg and
333 5 µg). Moreover, STB-EVs demonstrated a dose-dependent breakdown of kynurenine, as
334 evidenced by the significant reduction in kynurenine levels when 5 µg of STB-EVs was used
335 compared to 1 µg, in both incubation periods ($p < 0.05$ in both cases).

336 **Measurement of serum kynurenine**

337 Using GCxGC-MS, we investigated the serum levels of kynurenine in women with EOPE
338 (sFLT-1:PIGF ratio > 85) (n=9) and gestationally matched women with NP (sFLT-1:PIGF
339 ratio < 38) (n=9) (Fig 5). Women with EOPE exhibited significantly lower levels of
340 kynurenine compared with NP women ($p < 0.05$) (Fig 5B).

341 **Discussion**

342 In this study, we describe for the first time that STB-EVs cargo includes functional
343 kynurenine metabolising enzymes (KYNU, KMO and KAT-III). These enzymes breakdown
344 kynurenine, a biologically active metabolite known for its antioxidant, vasodilatory and
345 hypotensive effects. Despite no significant differences in the content of kynurenine
346 metabolising enzymes being found between NP and EOPE STB-EVs, serum levels of
347 kynurenine were significantly reduced in EOPE. While other possible causes of this
348 discrepancy must be considered, these findings suggest that STB-EVs may participate in the
349 regulation of circulating kynurenine levels in NP and EOPE. This is particularly true given
350 that circulating levels of STB-EVs are higher in EOPE^{15,16}. This dose effect may lead to
351 higher concentrations of kynurenine metabolising enzymes and subsequently to reduced

352 levels of kynurenine. Whether STB-EV-mediated kynurenine metabolism participates in the
353 cascade of placental, angiogenic or immunological defects observed in PE requires further
354 investigation.

355 During normal pregnancy, tryptophan metabolism to kynurenine is increased due to the
356 upregulation of placental indoleamine 2,3-dioxygenase (IDO) expression³⁹, which may play a
357 critical role in mediating immune tolerance^{40,41} and vascular remodelling in the maternal-
358 foetal interface^{42,43}. In PE placental culture, the culture media have been found to have
359 reduced kynurenine levels, which has been attributed to the reduced expression of the IDO
360 enzyme in the PE placenta²⁴. Based on existing literature, we hypothesized that STB-EVs
361 express functionally active KYNME in addition to placental expression. Since the STB layer
362 of the placenta is known to extrude extracellular vesicles into the circulation, we believe that
363 the enzymes expressed on the STB-EVs could scavenge circulating kynurenine and reduce
364 the levels of available circulating kynurenine.

365 Our study provided evidence of the presence of KYNME in the placental tissue through
366 immunohistochemistry and western blot in both NP and PE placentae. The
367 immunohistochemistry staining intensity was highest in the STB layer in both NP and EOPE
368 placentae. We discovered that KYNME was expressed in STB-EVs obtained from NP and
369 EOPE placental perfusions, and the expression levels were similar. However, previous
370 research by our group showed that PE placentae release significantly more STB-EVs per unit
371 of blood than NP¹⁶. Therefore, it is possible that the quantity of STB-EV carried KYNME per
372 unit of blood is also higher in PE than in NP. This hypothesis is at least partly supported by
373 our findings, which showed that kynurenine levels were significantly reduced when exposed
374 to a higher quantity of STB-EVs (carrying functional KYNME) derived from NP implying a
375 dose response relationship between STB-EVs and kynurenine levels. Furthermore, we

376 validated our findings by observing a significant reduction in serum kynurenine levels in
377 biochemically and clinically confirmed EOPE women compared to gestationally matched
378 controls.

379 Recent research has demonstrated that kynurenine replacement was effective in reversing
380 abnormal placentation and reducing the likelihood of developing PE in uni-nephrectomised
381 mice²⁵. Our research presents a novel approach to investigate the function of STB-EVs from
382 NP and PE in regulating kynurenine metabolism. For example, our findings indicate that
383 exposing kynurenine to STB-EVs denatured using 100% trifluoroacetic acid (TFA) results in
384 significantly higher levels of kynurenine. This opens the possibility of exploring the use of
385 specific inhibitors for individual kynurenine metabolizing enzymes to mitigate the breakdown
386 of kynurenine.

387 Despite the relevance of our findings, we acknowledge limitations in our study including the
388 small sample size in our analysis. In this study, we used relatively stringent criteria to define
389 EOPE, which was aimed to generate as homogenous a disease pathophysiology as is possible
390 in this complex condition. Recruitment was difficult with a distinct phenotype from its late
391 onset component (LOPE), not only due to clinical complications which are sometimes
392 emergent, but the relative rarity of EOPE in our institution, as it is in other institutions from
393 high income countries.

394 In conclusion, our research unveils functional KYNME expression in STB-EVs from NP and
395 PE patients, offering new insights into the clinical syndrome of preeclampsia. Our findings
396 raise important questions about the potential effectiveness of kynurenine replacement as a
397 strategy for managing preeclampsia and suggest that further investigation is needed to
398 explore the role of KYNME inhibitors in conjunction with kynurenine replacement as a better
399 alternative for managing the condition.

400 **Clinical perspective**

401 This study presents the first evidence of functional kynurenine metabolizing enzymes
402 (KYNME) associated with circulating syncytiotrophoblast-derived extracellular vesicles
403 (STB-EVs). Previous work by our group has shown that syncytiotrophoblasts in EOPE
404 patients shed a greater number of EVs^{15,16}, which translates to an increased concentration of
405 circulating KYNME per unit blood volume. This may potentially explain in part the observed
406 reduction in serum kynurenine levels in EOPE. Based on these findings, future research
407 should explore the therapeutic potential of co-administering specific KYNME inhibitors with
408 kynurenine replacement therapy to effectively elevate circulating kynurenine levels in EOPE
409 patients.

410 Furthermore, our in vitro data reveals a dose- and time-dependent breakdown of kynurenine
411 by STB-EVs. This opens a promising new avenue for the development of sensitive and
412 specific tools for detecting kynurenine metabolites as potential biomarkers of EOPE. Future
413 research efforts should explore the feasibility of utilizing these metabolites for early diagnosis
414 and disease monitoring in EOPE patients.

415 **Conflict of interest**

416 None to declare.

417 **Author contribution**

418 MV conceptualized the study and lead the research team. PL performed most of the
419 experiments in this manuscript. TA, MW, ZY and WZ performed selected experiments. SC
420 and MV were responsible for patient recruitment. PL, TA, BK, CE, WZ and MV edited the
421 manuscript. BK, SC and MV supervised the project. All co-authors approved the final version
422 of this manuscript.

423 Acknowledgements

424 We acknowledge senior research midwife Fenella Roseman and research midwife Lotoyah
425 Carty who kindly recruited the patients for the study.

426 References

- 427 1. Duley L. The Global Impact of Pre-eclampsia and Eclampsia. *Semin Perinatol.*
428 2009;33(3):130-137. doi:10.1053/j.semperi.2009.02.010
- 429 2. Hypertension in Pregnancy. *Obstetrics & Gynecology.* 2013;122(5):1122-1131.
430 doi:10.1097/01.AOG.0000437382.03963.88
- 431 3. Ness RB, Roberts JM. Heterogeneous causes constituting the single syndrome of
432 preeclampsia: A hypothesis and its implications. *Am J Obstet Gynecol.*
433 1996;175(5):1365-1370. doi:10.1016/S0002-9378(96)70056-X
- 434 4. Steegers EA, von Dadelszen P, Duvekot JJ, Pijnenborg R. Pre-eclampsia. *The Lancet.*
435 2010;376(9741):631-644. doi:10.1016/S0140-6736(10)60279-6
- 436 5. Brown MA, Magee LA, Kenny LC, et al. The hypertensive disorders of pregnancy:
437 ISSHP classification, diagnosis & management recommendations for international
438 practice. *Pregnancy Hypertens.* 2018;13. doi:10.1016/j.preghy.2018.05.004
- 439 6. Redman CWG, Sacks GP, Sargent IL. Preeclampsia: An excessive maternal
440 inflammatory response to pregnancy. *Am J Obstet Gynecol.* 1999;180(2):499-506.
441 doi:10.1016/S0002-9378(99)70239-5
- 442 7. Redman CW, Sargent IL, Staff AC. IFPA Senior Award Lecture: Making sense of pre-
443 eclampsia – Two placental causes of preeclampsia? *Placenta.* 2014;35.
444 doi:10.1016/j.placenta.2013.12.008
- 445 8. Redman CWG, Staff AC, Roberts JM. Syncytiotrophoblast stress in preeclampsia: the
446 convergence point for multiple pathways. *Am J Obstet Gynecol.* 2022;226(2):S907-
447 S927. doi:10.1016/j.ajog.2020.09.047
- 448 9. Awoyemi T, Cerdeira AS, Zhang W, et al. Preeclampsia and syncytiotrophoblast
449 membrane extracellular vesicles (STB-EVs). *Clin Sci.* 2022;136(24):1793-1807.
450 doi:10.1042/CS20220149
- 451 10. Baig S, Kothandaraman N, Manikandan J, et al. Proteomic analysis of human placental
452 syncytiotrophoblast microvesicles in preeclampsia. *Clin Proteomics.* 2014;11(1):40.
453 doi:10.1186/1559-0275-11-40
- 454 11. Dragovic RA, Collett GP, Hole P, et al. Isolation of syncytiotrophoblast microvesicles
455 and exosomes and their characterisation by multicolour flow cytometry and
456 fluorescence Nanoparticle Tracking Analysis. *Methods.* 2015;87:64-74.
457 doi:10.1016/j.ymeth.2015.03.028
- 458 12. Awoyemi T, Motta-Mejia C, Zhang W, et al. Syncytiotrophoblast Extracellular
459 Vesicles From Late-Onset Preeclampsia Placentae Suppress Pro-Inflammatory

- 460 Immune Response in THP-1 Macrophages. *Front Immunol.* 2021;12.
461 doi:10.3389/fimmu.2021.676056
- 462 13. Lv Y, Tan J, Miao Y, Zhang Q. The role of microvesicles and its active molecules in
463 regulating cellular biology. *J Cell Mol Med.* 2019;23(12):7894-7904.
464 doi:10.1111/jcmm.14667
- 465 14. Théry C. Exosomes: secreted vesicles and intercellular communications. *F1000 Biol*
466 *Rep.* 2011;3. doi:10.3410/B3-15
- 467 15. Knight M, Redman CWG, Linton EA, Sargent IL. Shedding of syncytiotrophoblast
468 microvilli into the maternal circulation in pre-eclamptic pregnancies. *BJOG.*
469 1998;105(6):632-640. doi:10.1111/j.1471-0528.1998.tb10178.x
- 470 16. Goswami D, Tannetta DS, Magee LA, et al. Excess syncytiotrophoblast microparticle
471 shedding is a feature of early-onset pre-eclampsia, but not normotensive intrauterine
472 growth restriction. *Placenta.* 2006;27(1). doi:10.1016/j.placenta.2004.11.007
- 473 17. Gardiner C, Tannetta DS, Simms CA, Harrison P, Redman CWG, Sargent IL.
474 Syncytiotrophoblast Microvesicles Released from Pre-Eclampsia Placentae Exhibit
475 Increased Tissue Factor Activity. *PLoS One.* 2011;6(10):e26313.
476 doi:10.1371/journal.pone.0026313
- 477 18. Ribeiro MF, Zhu H, Millard RW, Fan GC. Exosomes Function in Pro- and Anti-
478 Angiogenesis. *Curr Angiogenes.* 2013;2(1):54-59.
479 doi:10.2174/22115528113020020001
- 480 19. Guller S, Tang Z, Ma YY, Di Santo S, Sager R, Schneider H. Protein composition of
481 microparticles shed from human placenta during placental perfusion: Potential role in
482 angiogenesis and fibrinolysis in preeclampsia. *Placenta.* 2011;32(1):63-69.
483 doi:10.1016/j.placenta.2010.10.011
- 484 20. Worton SA, Pritchard HAT, Greenwood SL, et al. Kynurenine Relaxes Arteries of
485 Normotensive Women and Those With Preeclampsia. *Circ Res.* 2021;128(11):1679-
486 1693. doi:10.1161/CIRCRESAHA.120.317612
- 487 21. Rios C, Santamaria A. Quinolinic acid is a potent lipid peroxidant in rat brain
488 homogenates. *Neurochem Res.* 1991;16(10). doi:10.1007/BF00966592
- 489 22. Wang Y, Liu H, McKenzie G, et al. Kynurenine is an endothelium-derived relaxing
490 factor produced during inflammation. *Nat Med.* 2010;16(3). doi:10.1038/nm.2092
- 491 23. Sakakibara K, Feng GG, Li J, et al. Kynurenine causes vasodilation and hypotension
492 induced by activation of KCNQ-encoded voltage-dependent K⁺ channels. *J*
493 *Pharmacol Sci.* 2015;129(1). doi:10.1016/j.jphs.2015.07.042
- 494 24. Dunn WB, Brown M, Worton SA, et al. Changes in the Metabolic Footprint of
495 Placental Explant-Conditioned Culture Medium Identifies Metabolic Disturbances
496 Related to Hypoxia and Pre-Eclampsia. *Placenta.* 2009;30(11).
497 doi:10.1016/j.placenta.2009.08.008
- 498 25. Dupont V, Berg AH, Yamashita M, et al. Impaired renal reserve contributes to
499 preeclampsia via the kynurenine and soluble fms-like tyrosine kinase 1 pathway.
500 *Journal of Clinical Investigation.* Published online August 9, 2022.
501 doi:10.1172/JCI158346

- 502 26. Levine RJ, Maynard SE, Qian C, et al. Circulating Angiogenic Factors and the Risk of
503 Preeclampsia. *New England Journal of Medicine*. 2004;350(7).
504 doi:10.1056/NEJMoa031884
- 505 27. Bender DA. Biochemistry of tryptophan in health and disease. *Mol Aspects Med*.
506 1983;6(2):101-197. doi:10.1016/0098-2997(83)90005-5
- 507 28. Badawy AAB. Tryptophan Metabolism in Alcoholism. In: ; 1999:265-274.
508 doi:10.1007/978-1-4615-4709-9_33
- 509 29. Kudo Y, Boyd CAR, Sargent IL, Redman CWG. Decreased tryptophan catabolism by
510 placental indoleamine 2,3-dioxygenase in preeclampsia. *Am J Obstet Gynecol*.
511 2003;188(3). doi:10.1067/mob.2003.156
- 512 30. Badawy AAB. Kynurenine pathway of tryptophan metabolism: Regulatory and
513 functional aspects. *International Journal of Tryptophan Research*. 2017;10(1).
514 doi:10.1177/1178646917691938
- 515 31. Cerdeira AS, O'Sullivan J, Ohuma EO, et al. Randomized Interventional Study on
516 Prediction of Preeclampsia/Eclampsia in Women With Suspected Preeclampsia.
517 *Hypertension*. 2019;74(4). doi:10.1161/HYPERTENSIONAHA.119.12739
- 518 32. Dragovic RA, Collett GP, Hole P, et al. Isolation of syncytiotrophoblast microvesicles
519 and exosomes and their characterisation by multicolour flow cytometry and
520 fluorescence Nanoparticle Tracking Analysis. *Methods*. 2015;87:64-74.
521 doi:10.1016/j.ymeth.2015.03.028
- 522 33. Jiang S, Zhang W, Cao Q, et al. ExoCounter Assays Identify Women Who May
523 Develop Early-Onset Preeclampsia From 12.5 μ L First-Trimester Serum by
524 Characterizing Placental Small Extracellular Vesicles. *Hypertension*. 2023;80(7):1439-
525 1451. doi:10.1161/HYPERTENSIONAHA.123.20907
- 526 34. Awoyemi T, Jiang S, Rahbar M, et al. MicroRNA analysis of medium/large placenta
527 extracellular vesicles in normal and preeclampsia pregnancies. *Front Cardiovasc Med*.
528 2024;11. doi:10.3389/fcvm.2024.1371168
- 529 35. Awoyemi T, Zhang W, Rahbar M, et al. A cross-sectional analysis of
530 syncytiotrophoblast membrane extracellular vesicles-derived transcriptomic
531 biomarkers in early-onset preeclampsia. *Front Cardiovasc Med*. 2023;10.
532 doi:10.3389/fcvm.2023.1291642
- 533 36. Théry C, Witwer KW, Aikawa E, et al. Minimal information for studies of
534 extracellular vesicles 2018 (MISEV2018): a position statement of the International
535 Society for Extracellular Vesicles and update of the MISEV2014 guidelines. *J*
536 *Extracell Vesicles*. 2018;7(1):1535750. doi:10.1080/20013078.2018.1535750
- 537 37. Yu Z, Huang H, Zhang H, Kessler BM. Improved profiling of polyamines using two-
538 dimensional gas chromatography mass spectrometry. *Talanta*. 2019;199:184-188.
539 doi:10.1016/j.talanta.2019.02.062
- 540 38. Yu Z, Huang H, Reim A, et al. Optimizing 2D gas chromatography mass spectrometry
541 for robust tissue, serum and urine metabolite profiling. *Talanta*. 2017;165:685-691.
542 doi:10.1016/j.talanta.2017.01.003
- 543 39. Broekhuizen M, Danser AHJ, Reiss IKM, Merkus D. The Function of the Kynurenine
544 Pathway in the Placenta: A Novel Pharmacotherapeutic Target? *Int J Environ Res*
545 *Public Health*. 2021;18(21):11545. doi:10.3390/ijerph182111545

- 546 40. Munn DH, Zhou M, Attwood JT, et al. Prevention of allogeneic fetal rejection by
547 tryptophan catabolism. *Science*. 1998;281(5380):1191-1193.
548 doi:10.1126/science.281.5380.1191
- 549 41. Munn DH, Shafizadeh E, Attwood JT, Bondarev I, Pashine A, Mellor AL. Inhibition
550 of T Cell Proliferation by Macrophage Tryptophan Catabolism. *J Exp Med*.
551 1999;189(9):1363-1372. doi:10.1084/jem.189.9.1363
- 552 42. Zardoya-Laguardia P, Blaschitz A, Hirschmugl B, et al. Endothelial indoleamine 2,3-
553 dioxygenase-1 regulates the placental vascular tone and is deficient in intrauterine
554 growth restriction and pre-eclampsia. *Sci Rep*. 2018;8(1):5488. doi:10.1038/s41598-
555 018-23896-0
- 556 43. Broekhuizen M, Klein T, Hitzerd E, et al. Tryptophan-Induced Vasodilation Is
557 Enhanced in Preeclampsia. *Hypertension*. 2020;76(1):184-194.
558 doi:10.1161/HYPERTENSIONAHA.120.14970

559

560 **Table legend**

561 **Table 1. Clinical characteristics of studied women.**

562 Note: Values presented as mean \pm SD. SBP, systolic blood pressure. DPB, diastolic blood
563 pressure. BMI, body mass index (kg/m^2).

564

565 **Figure legend.**

566 **Figure 1. Characterization of large/medium and small STB-EVs isolated from normal**
567 **pregnancies. A)** Representative characterization of medium/large STB-EVs, and **B)** small
568 STB-EVs by NTA. Inserted images are representative pictures of respective STB-EVs
569 characterized by TEM. Right, scale bar = 1000 nm. Left, scale bar = 2 μm . White square
570 represent section amplified. N=3 per group. **C)** Representative images of Western blot for
571 detecting placental origin of STB-EVs. Placental alkaline phosphatase (PLAP) was used as
572 placental marker. CD63, CD9 and Alix were used as positive marker of EVs. Cytochrome C
573 (CYT.C) was used as negative marker of EVs.

574

575 **Figure 2. Placental protein expression of kynurenine metabolising enzymes (KYNME).**

576 **A)** Placental lysates obtained from normal pregnancy (NP, n=3) and preeclamptic
577 pregnancies (EOPE, n=3) probed for KYNME and placental alkaline phosphatase (PLAP).
578 HEPG2 cell lysate used as positive control. **B)** Immunohistochemistry analysis of placental
579 expression of Anti KYNU (1); Anti KAT III (2) and Anti KMO (3) in NP and EOPE
580 placentas. Arrows indicate presence of these proteins in the syncytiotrophoblast cells.

581

582 **Figure 3. KYNMEs are expressed by STB-EVs isolated from normal and preeclamptic**
583 **pregnancies. A)** Representative images of capillary electrophoresis of KYNME including
584 KYNU, KMO, and KAT-III in STB-EVs extracted from normal (NP, n=3) and preeclamptic
585 pregnancies (EOPE, n=3). Placental alkaline phosphatase (PLAP) was used as placental
586 marker. Liver cell and placental lysates were used as respective positive and negative
587 controls. **B)** Relative values of KYNMEs after normalizing for total protein. NS, non-
588 statistical significance. Values are presented as mean \pm SD.

589

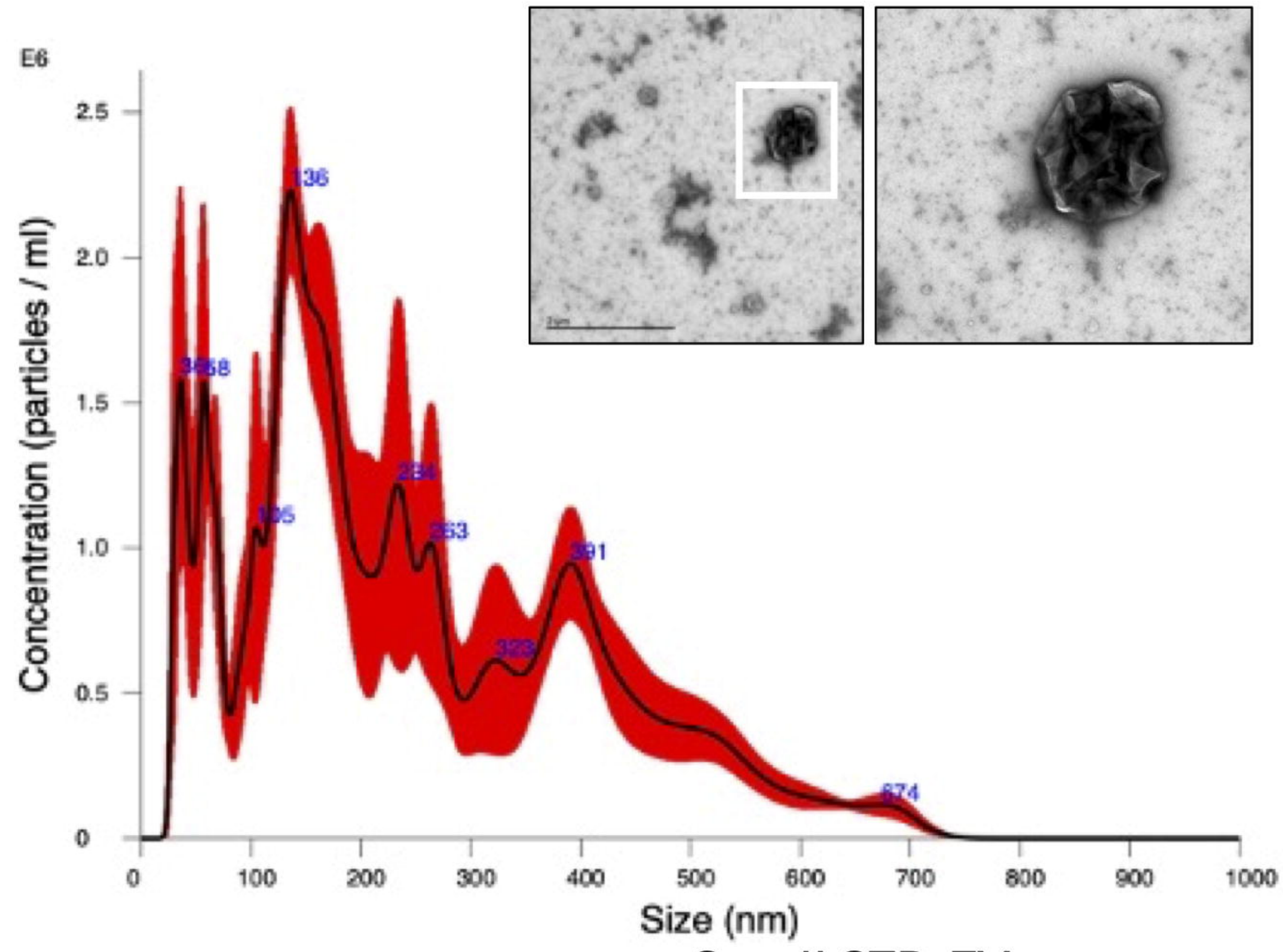
590 **Figure 4. STB-EVs isolated from normal pregnancy break down kynurenine. A)**
591 Percentage of kynurenine metabolized with STB-EVs (1 μ g, red bar; and 5 μ g, green bar, of
592 total protein) isolated from normal pregnancy placentae (n=3). Two different incubation time
593 were tested. **B)** 5 min, and **C)** 60 min of incubation with STB-EVs. Denatured STB-EVs
594 (using 100% trifluoroacetic acid) were used as control. Each dot represents an individual STB-
595 EV extraction. Values are presented as mean \pm SD. *p* value is indicated in each comparison.

596

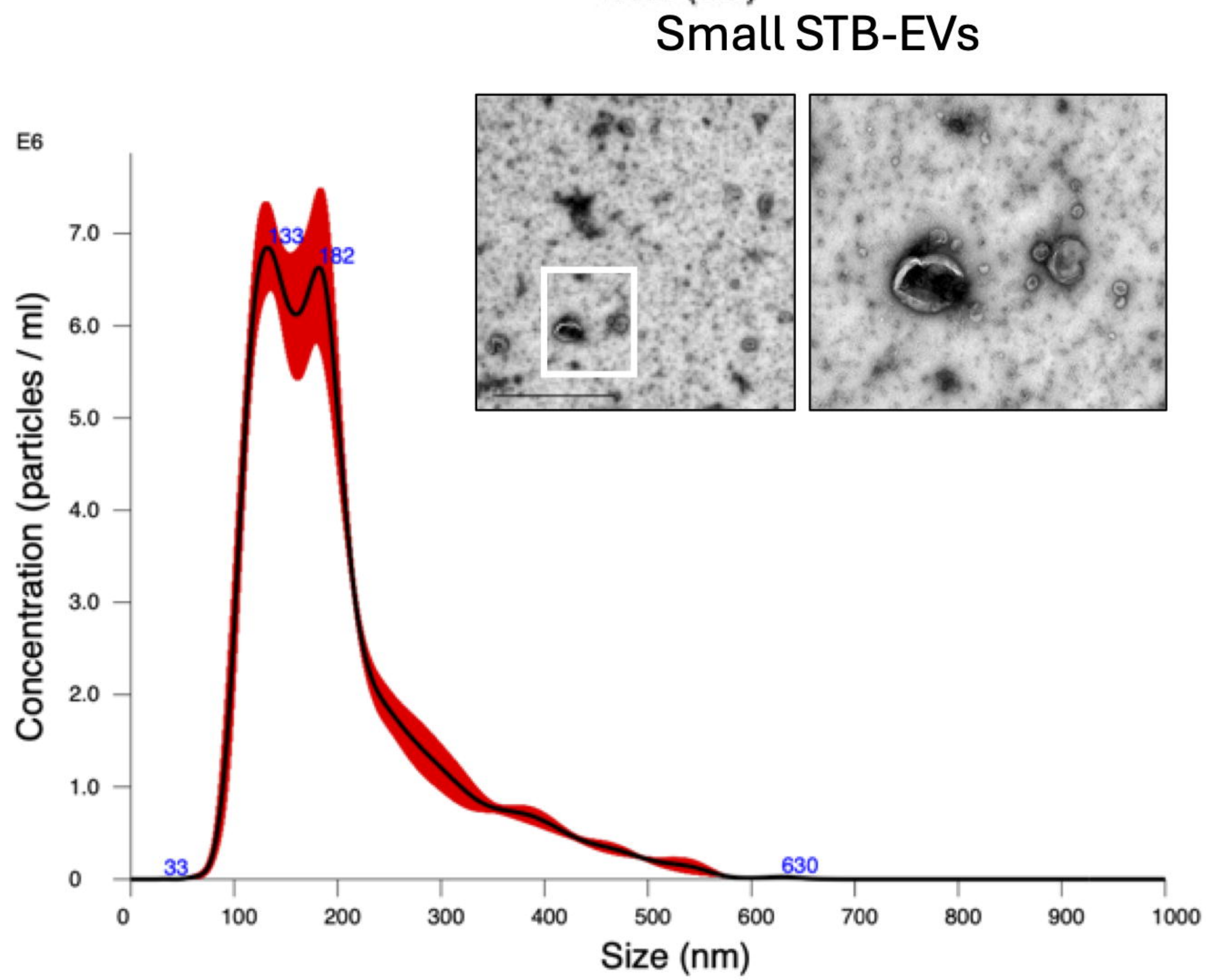
597 **Figure 5. Serum kynurenine levels in normal and preeclamptic pregnancies. A)**
598 Representative chart of gas chromatography mass spectrometry for kynurenine (KYN)
599 detection in serum from normal (NP, n=9, pink) and preeclamptic pregnancies (EOPE, n=9,
600 blue). As a control we used an in-house library of KYN (black). **B)** Amplification of the
601 chromatogram in which KYN is detected. Notice the differences in the peak generated in NP
602 and EOPE samples. **C)** KYN levels presented as mean \pm SD. Each dot represents an
603 individual. *p* value is indicated in each comparison.

Medium/Large STB-EVs

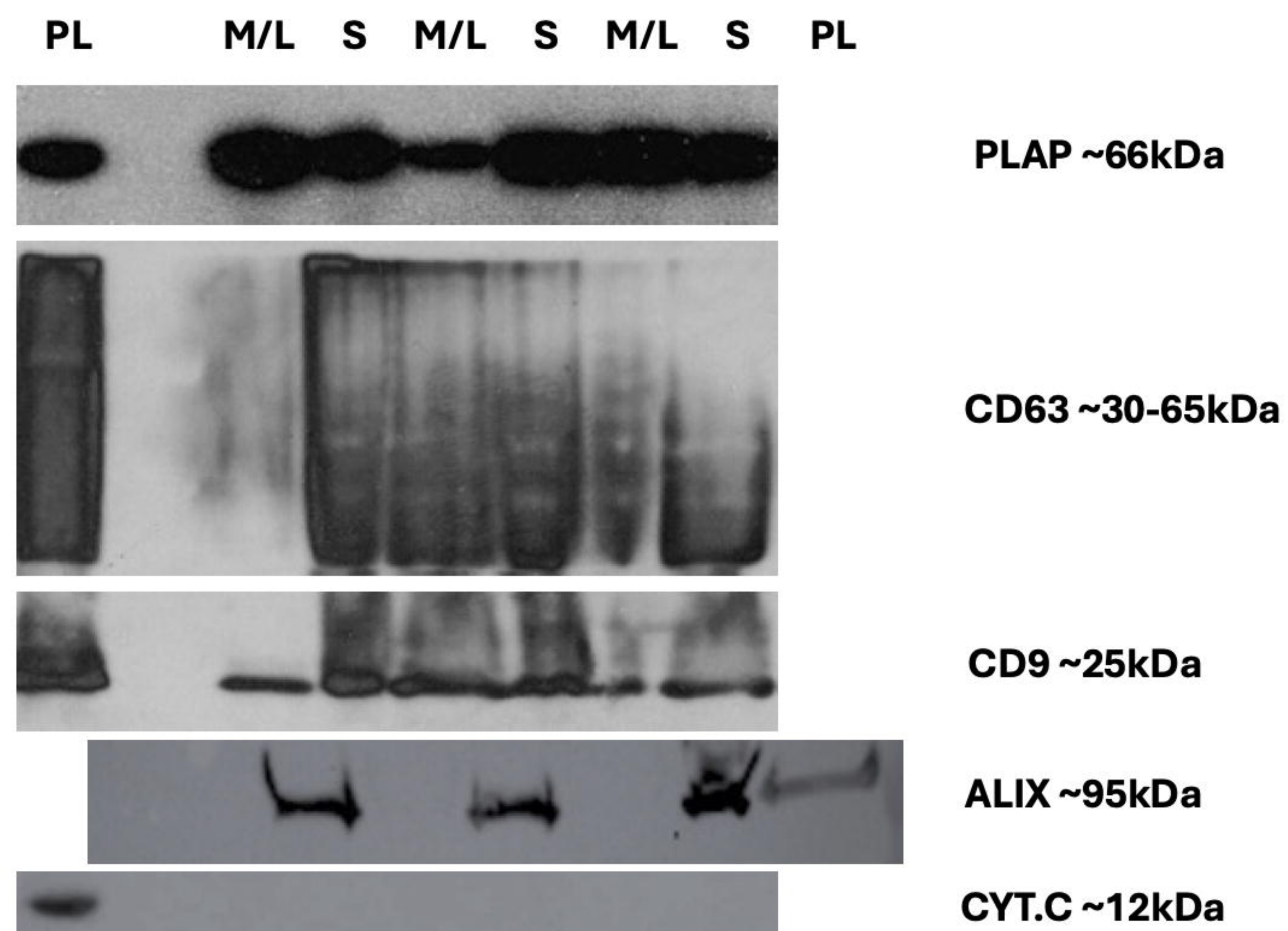
A

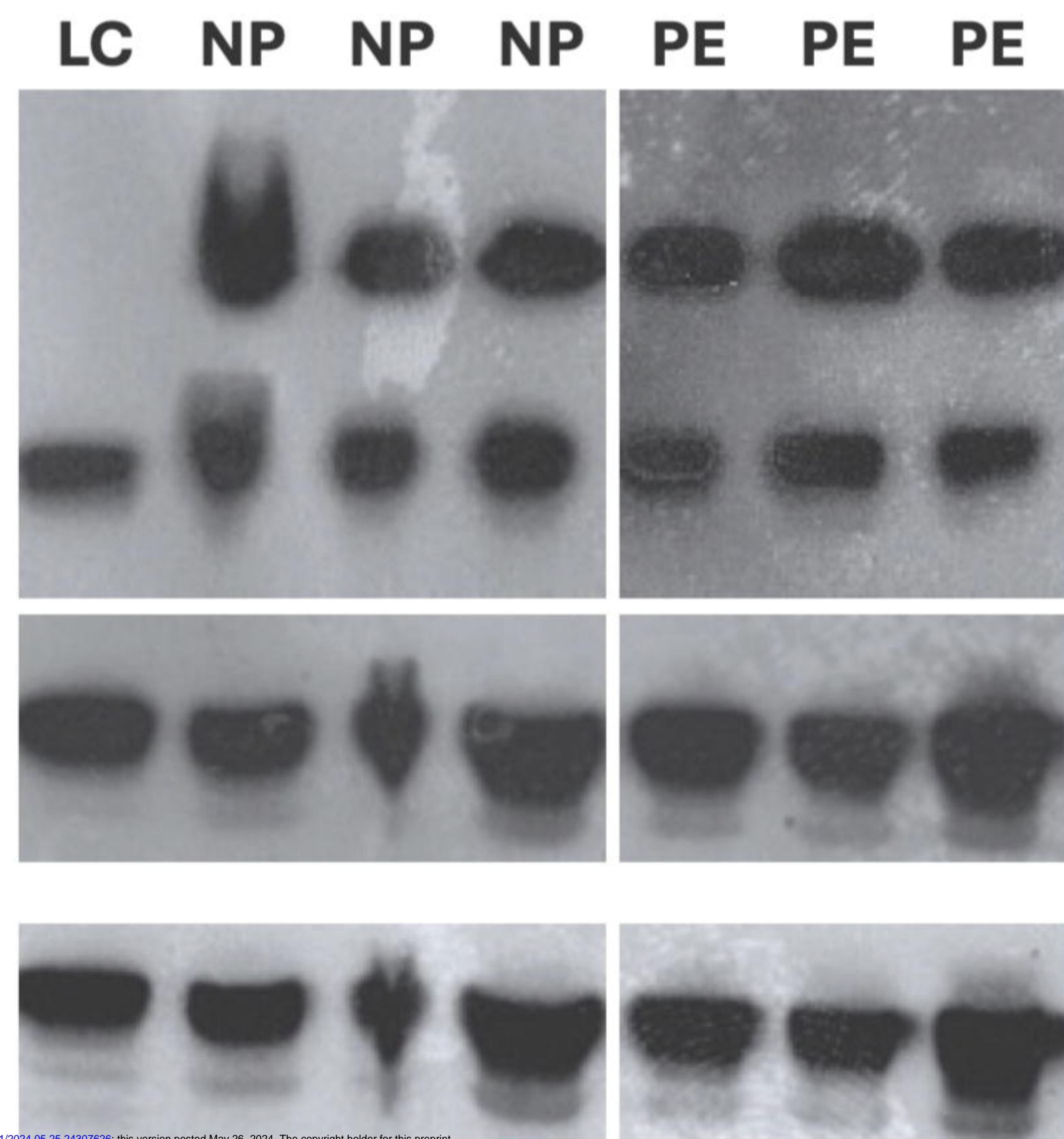


B

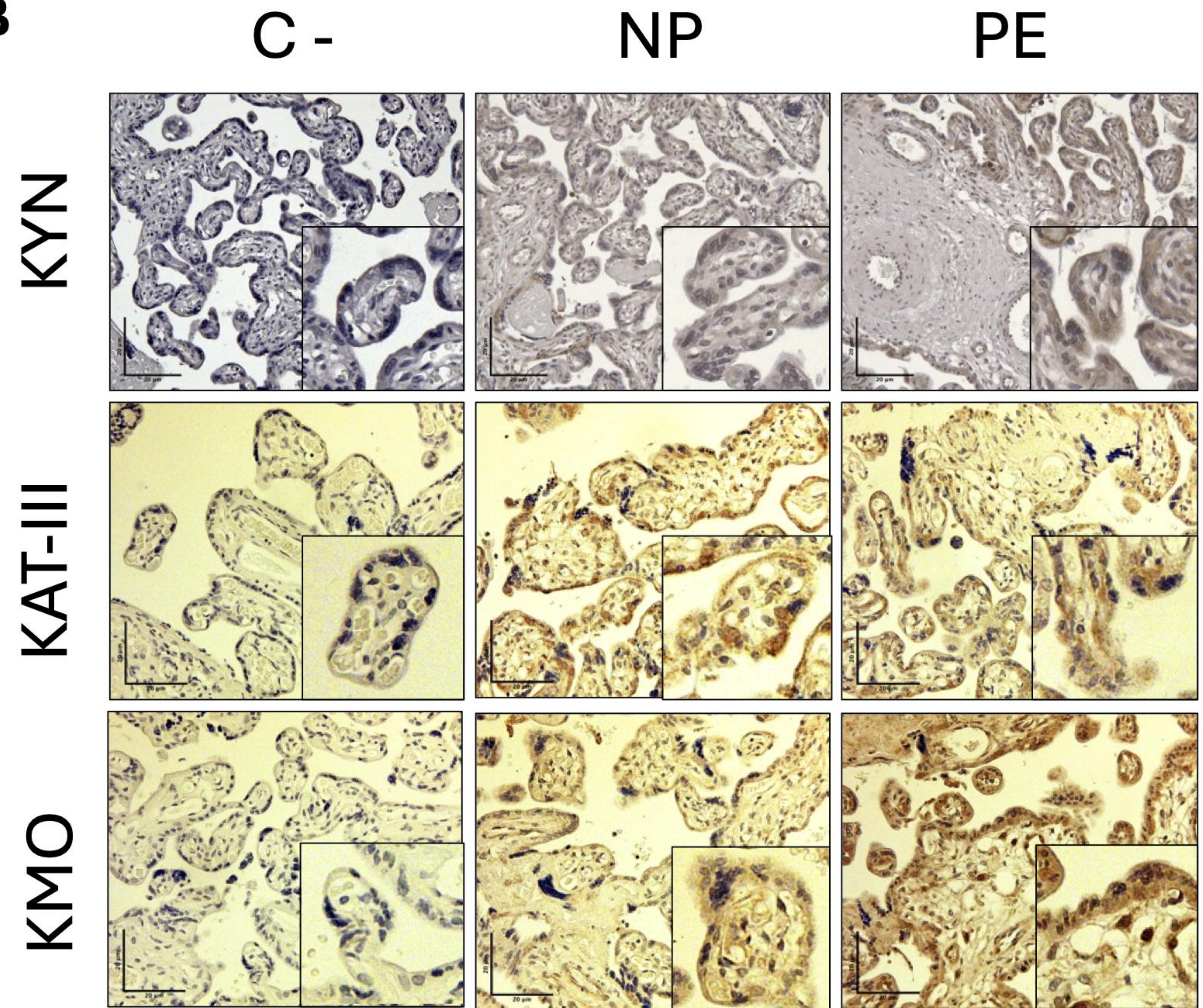


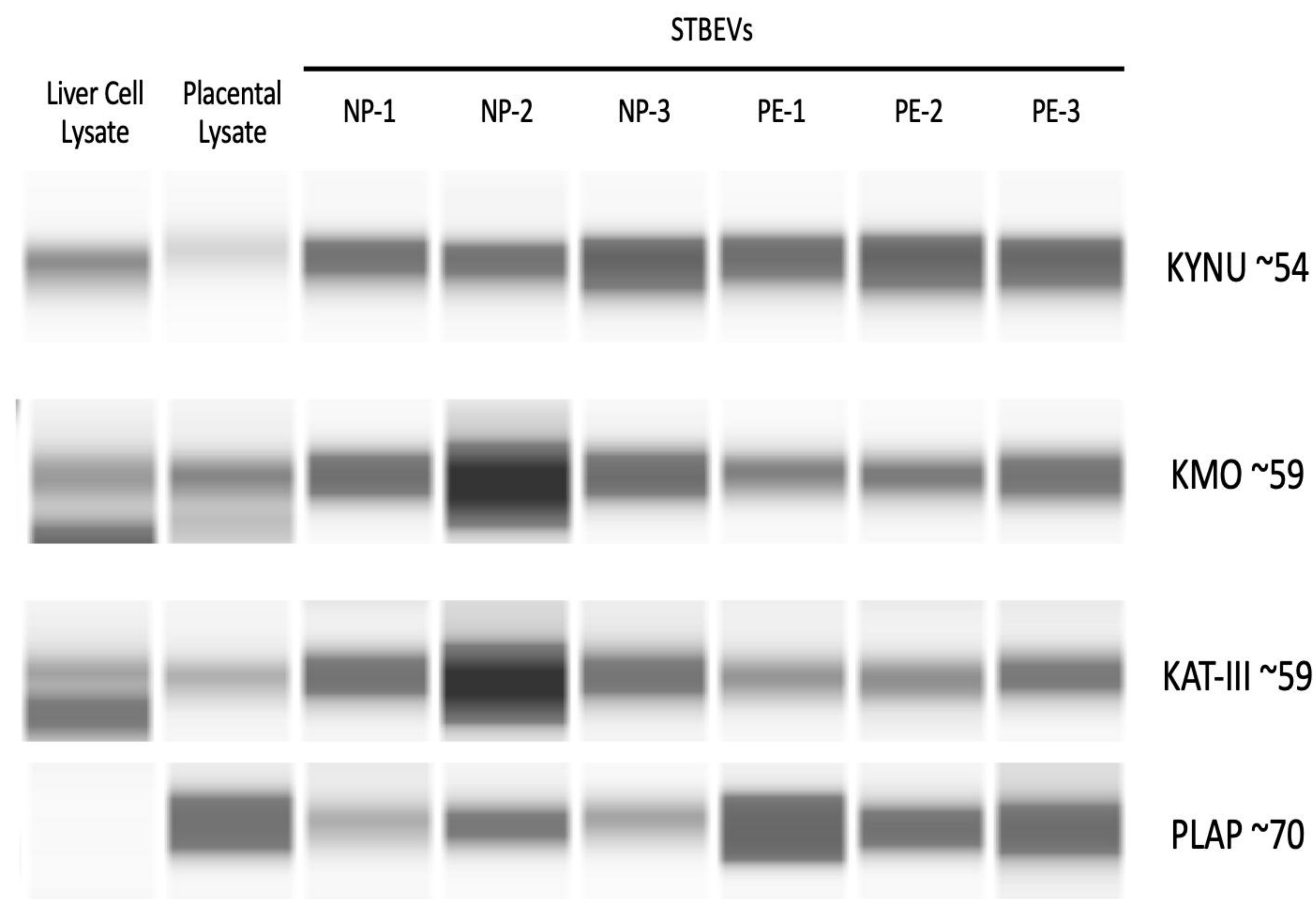
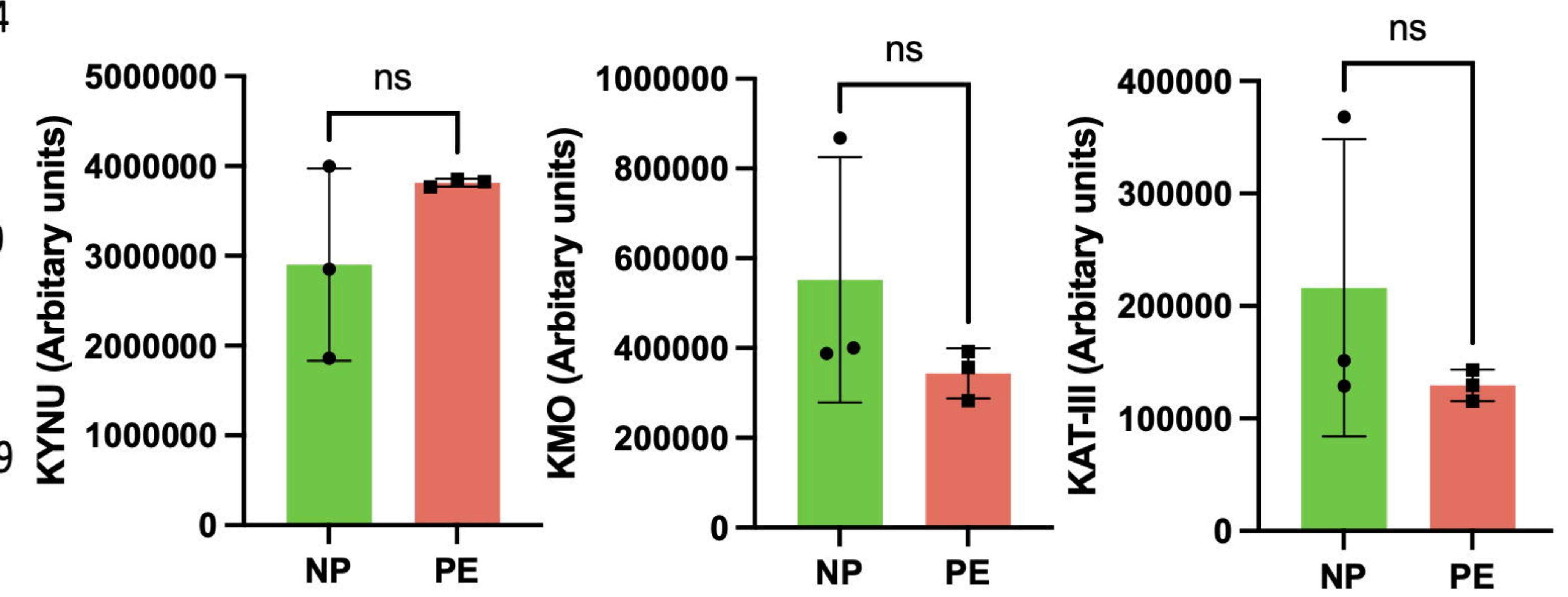
C



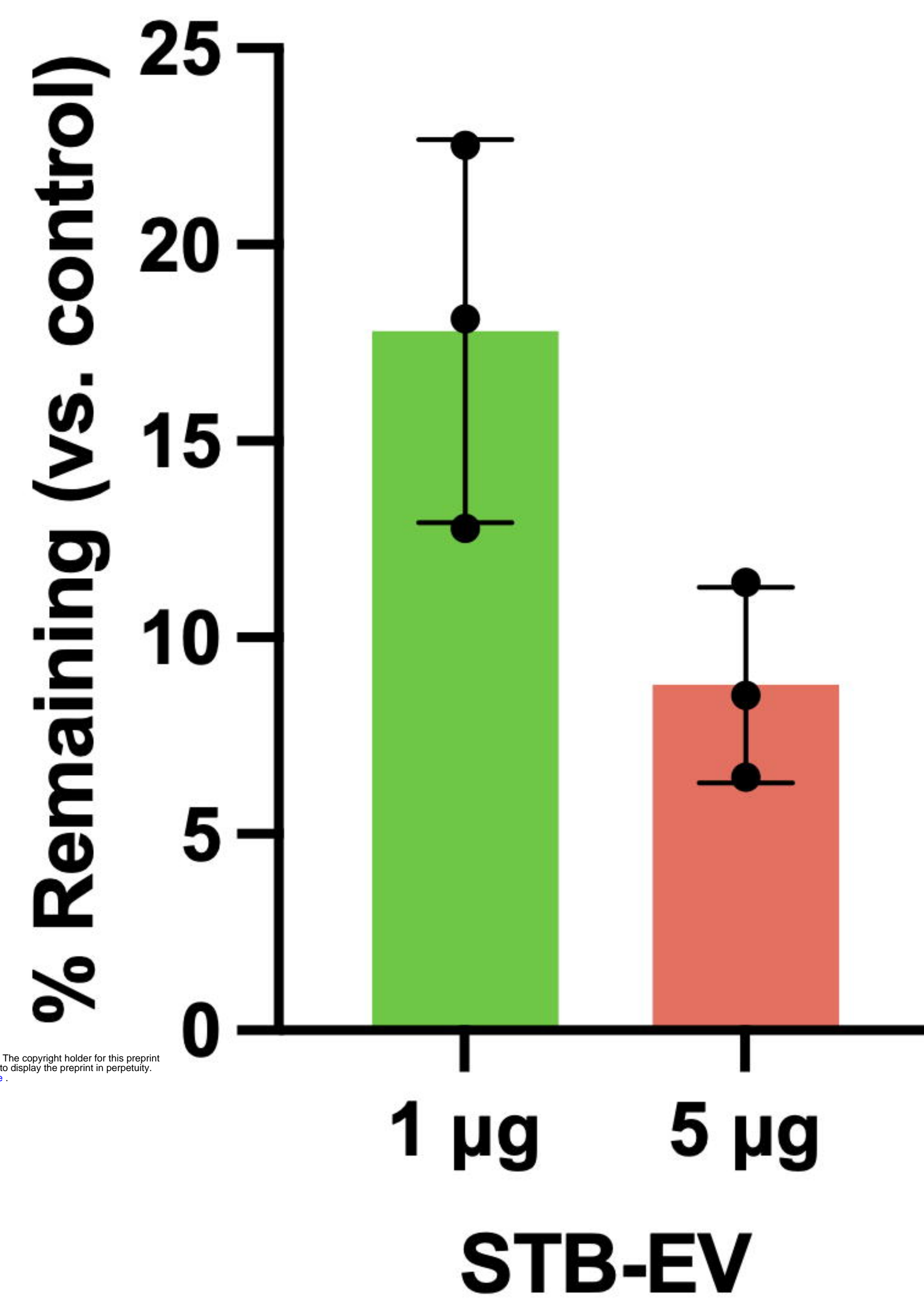
A

medRxiv preprint doi: <https://doi.org/10.1101/2024.05.20.24267820>; this version posted May 20, 2024. The copyright holder for this preprint (which was not certified by peer review) is the author/funder, who has granted medRxiv a license to display the preprint in perpetuity. It is made available under a CC-BY-NC-ND 4.0 International license.

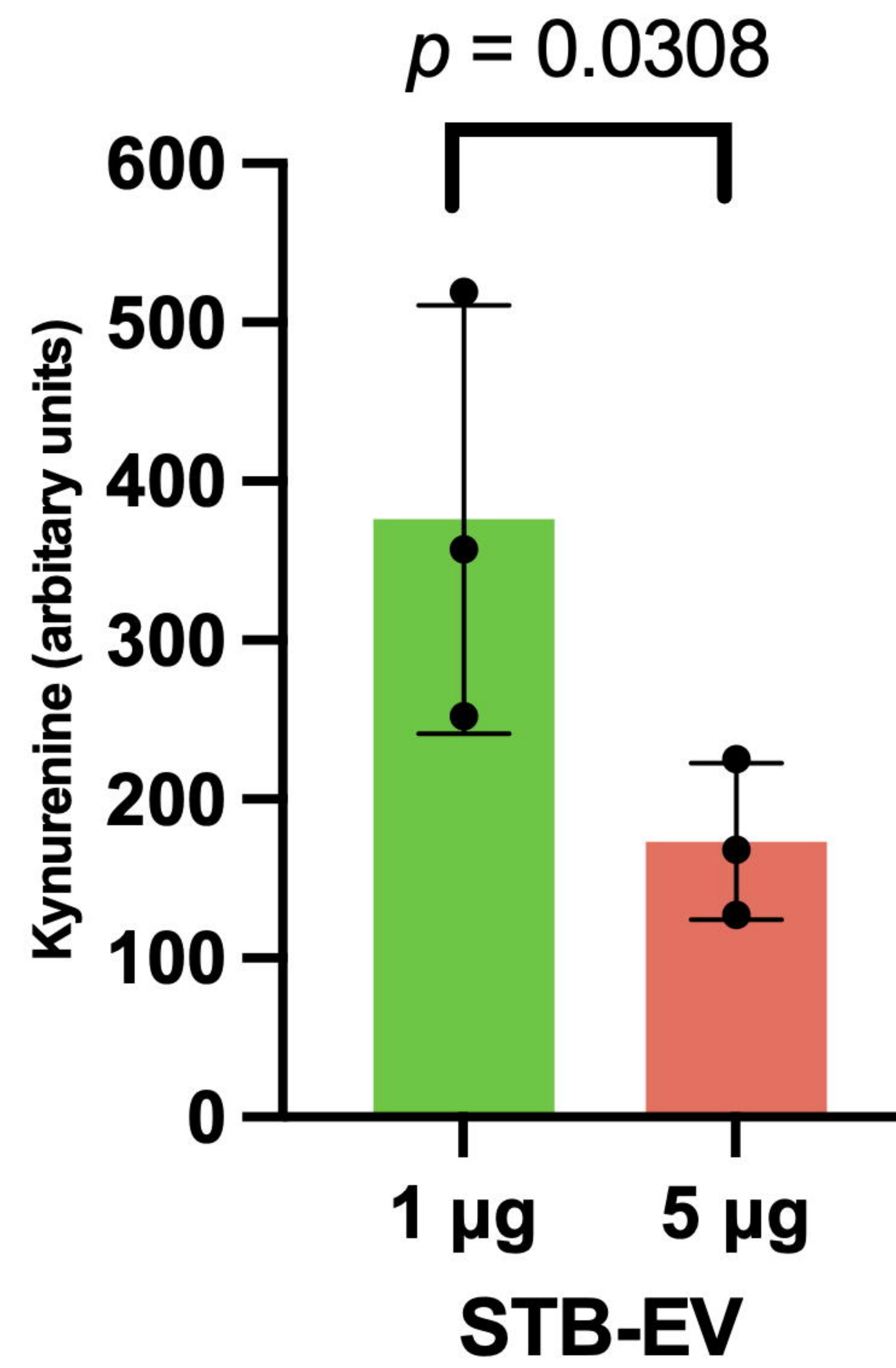
B

A**B**

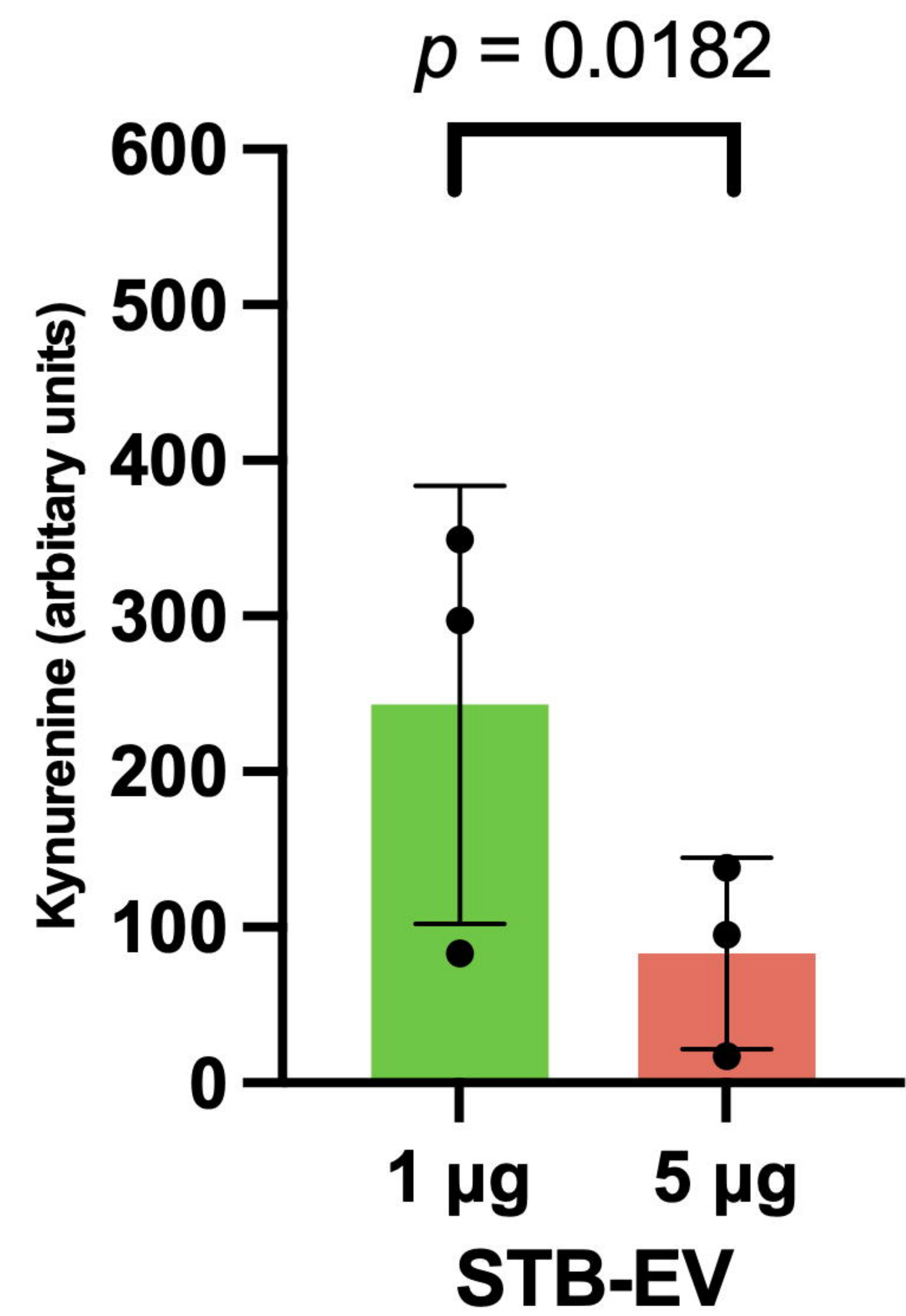
A 5 minutes

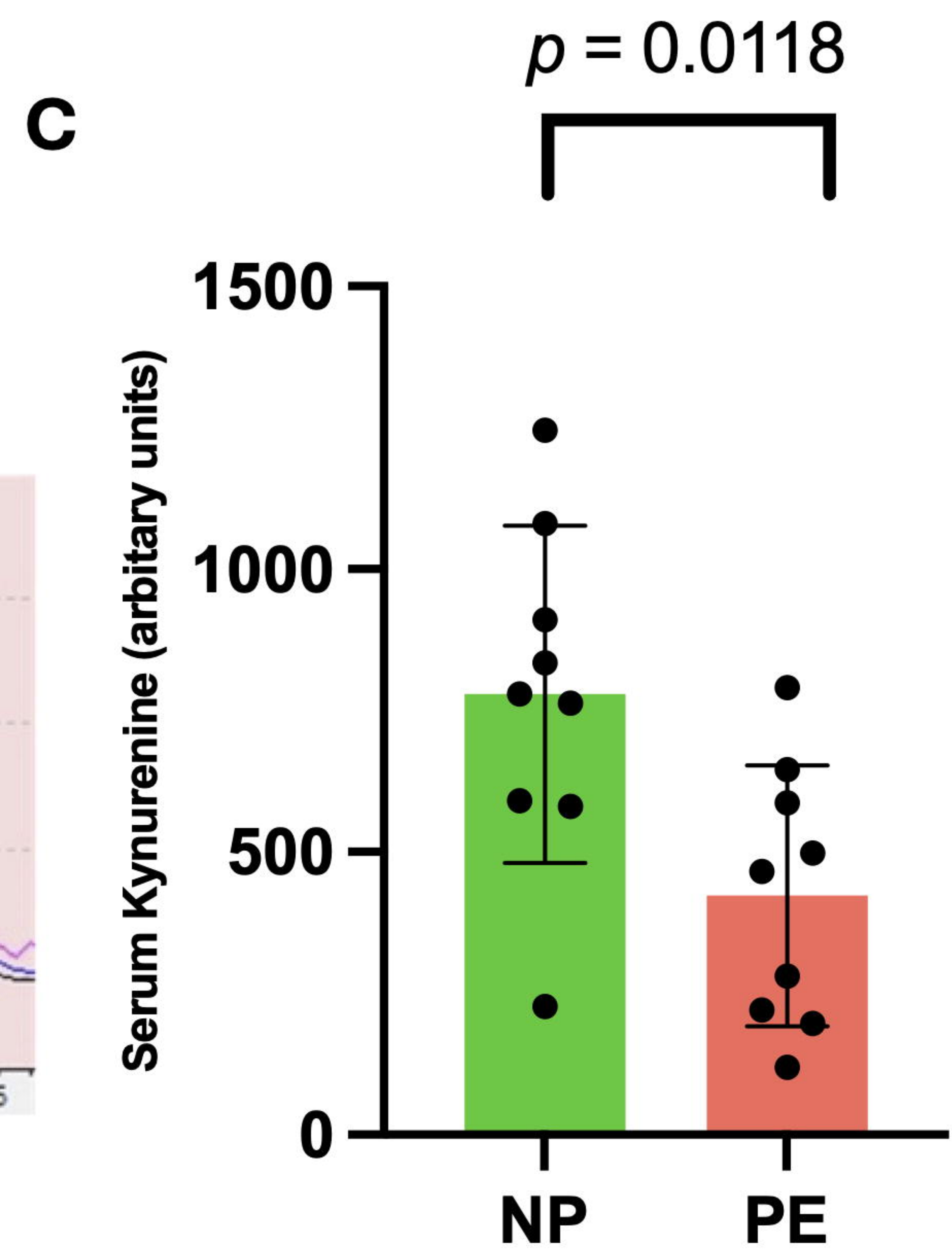
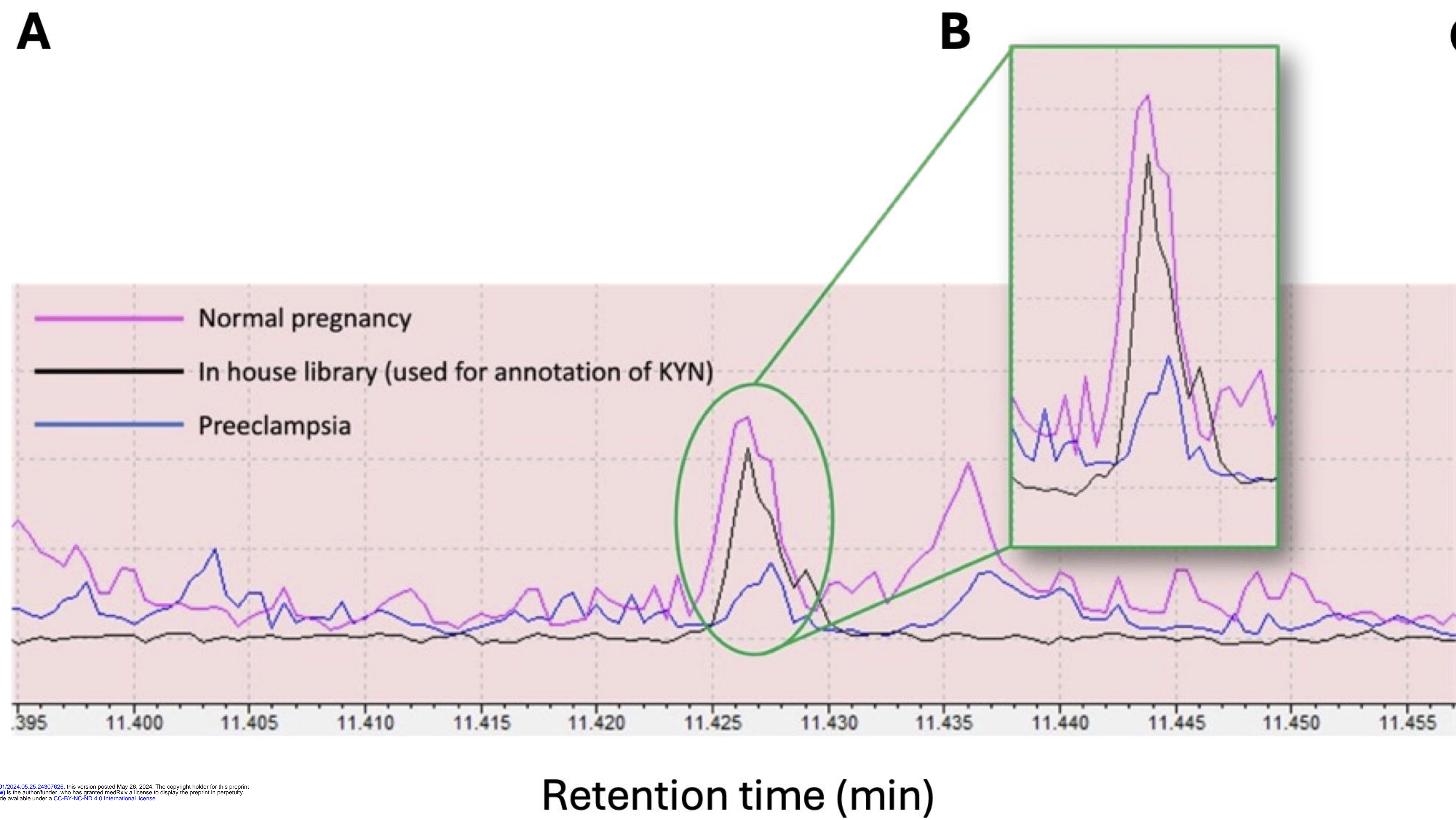


B 5 minutes



C 60 minutes





medRxiv preprint doi: <https://doi.org/10.1101/2024.05.20.24267626>; this version posted May 20, 2024. The copyright holder for this preprint (which was not certified by peer review) is the author/funder, who has granted medRxiv a license to display the preprint in perpetuity. It is made available under a CC-BY-NC-ND 4.0 International license.

Table 1. Clinical characteristics of studied women.

	NP (n=9)	EOPE (n=9)	P value
Age (years)	28.6 ± 4.2	30.4 ± 4.1	> 0.05
Gestational age (weeks)	28.3 ± 2.9	28.0 ± 2.7	> 0.05
SBP (mmHg)	111.3 ± 7.5	156.3 ± 14.6	< 0.0001
DBP (mmHg)	67.3 ± 6.1	100.8 ± 6.6	< 0.0001
BMI (kg/m ²)	24.2 ± 4.0	29.1 ± 7.6	> 0.05
Birth weight (g)	3801 ± 666.3	1815 ± 527.5	< 0.0001
Gestation at delivery (weeks)	39.0 ± 1.3	32.3 ± 2.7	< 0.0001
sFlt-1:PlGF	1.0 ± 0.2	599.3 ± 569.5	< 0.05

Note: Values are presented mean ± SD. SBP, systolic blood pressure. DPB, diastolic blood pressure. BMI, body mass index (kg/m²).